Egyptian Journal of Veterinary Sciences

https://ejvs.journals.ekb.eg/

Dysregulation of Hepatic AMPK and SIRT-1 Expressions Mediates Aluminum Oxide Nanoparticles-Induced Hepatic Injury and Microangiopathy in Rats with Special Emphasis on Shape-Dependent Hepatotoxicity

Esraa M. Hegazy[1], Mohamed Y. Mahmoud[2], Faten F. Mohammed[1,3] and Magdy M. El-Mahdy [1]

[1]*Pathology Department, Faculty of Veterinary Medicine, Cairo University, Giza 12211, Egypt.*
[2] *Toxicology and Forensic Medicine Department, Faculty of Veterinary Medicine, Cairo University, Giza 12211, Egypt.*
[3]*Department of Pathology, College of Veterinary Medicine, King Faisal University, AlAhsa, 31982, Saudi Arabia.*

Abstract

ALUMINUM oxide (Al_2O_3) nanoparticles (NPCs) are widely used in various medical purposes, including drug delivery; thus, the safety evaluation of their toxicity is crucial. The present study aimed to evaluate the hepatotoxic potential of Al_2O_3 nanoparticles in rats and clarify the molecular pathways that mediate their effect. The oral intoxication of rats with two different shapes of Al_2O_3 NPCs (nanoparticles spheres-NPS) and nanoparticles rods-NPRs) were performed, the doses were 20 mg and 40 mg/kg b.w. daily for 2 months. At the end of the experimental period, blood and liver samples were collected to determine liver biochemical enzymes and oxidative stress markers, in addition to histopathological evaluation of the liver. The immunohistochemical characterization of AMPK and SIRT-1 was also investigated. Results revealed that Al_2O_3 NPCs induced a significant increase in hepatic enzymes and oxidative stress parameters in a dose-dependent manner, severe histopathological hepatic alterations, including macro- to microvesicular hepatic steatosis, hepatocellular necrosis, in addition to severe portal reactions characterized by microangiopathy with portal cholangiofibrosis. Downregulation of AMPK and SIRT-1 expression in hepatic parenchyma was evident. Conclusion: The present study confirmed that aluminum nanoparticles have hepatotoxic potential in rats through the induction of oxidative stress and the downregulation of AMPK and SIRT-1.

Keywords: Aluminum oxide, Nanoparticles, liver, Sirt-1, AMPK, rat.

Introduction

Metal oxide nanoparticles (MONPs) are inorganic materials that have become a valuable tool for many industrial sectors, especially in healthcare, due to their versatility, unique intrinsic properties, and relatively inexpensive production cost. Because of their wide applications in biology and medicine, for example, nano-metals and their oxides, such as Nano-silver, nano-copper, and nano-zinc, are gradually applied in biomedical fields such as medical antibacterial, cancer treatment, and other clinical fields [1].

Metallic nanoparticles (silver, gold, and silver–gold alloy nanoparticles) with their unique properties play a significant role in preventing blood clot formation, dissolution of blood clots, and enhanced thrombus (blood clot) imaging in vivo [2], so human exposure to MONPs has increased dramatically. This requires these materials to undergo laboratory experiments.

*Corresponding authors: Faten F. Mohammed, E-mail:fatenfathy21@yahoo.com, faten.fathy@cu.edu.eg, fhanafi@kfu.edu.sa, Tel:+02 01003542636
(Received 10 July 2025, accepted 19 September 2025)
DOI: 10.21608/EJVS.2025.401975.2960

One of the materials that received our attention due to the spread of its use is Aluminum oxide nanoparticles (Al_2O_3 NPs). Various studies have focused on using Al_2O_3 NPs to improve the targeting of vaccines, increasing cellular uptake, and improving permeability and efficacy [3]. The application of Al_2O_3 NPs in cancer therapy has been studied due to the powerful induction of a cellular immune response by Al_2O_3 NPs. A recent study showed exceeding performance in anti-tumor vaccine design based on Al_2O_3 NPs [4]. Other uses include biomolecular preservation and stabilization, Industrial production as gas sensors, and medical sensors.[5&6]

ALNPs have toxic effects on different body systems, including the nervous system, hepatorenal, reproductive, and musculoskeletal through oxidative stress, inflammation, genotoxic effects, and depletion of the antioxidant system. The toxicologic effects of ALNPs included neuroinflammation and Alzheimer's disease, hepatorenal dysfunction, reduction in sperm quality, and impairment in bone mineralization. [7,8,9].

The potential cytotoxic effect of nanoparticles (NPCs) depends upon the interaction of NPCs with the cells; the aspect ratio of the particle determines cellular uptake and toxicity, and the longer and thinner the particle, the more toxic the potential, while the larger the aspect ratio, the more decreased cellular uptake and toxicity result [10]. In this aspect, the long rod non-functionalized particles between 15 and 30 nm, thickness assumed to be slightly cytotoxic. The spherical-shaped aluminum oxide nanoparticles have a greater surface area and a more toxic effect [11]. Previous studies have focused on the effect of the shape of NPCs on their toxicities; Dong et al. [12]. stated that nanorods had more adverse effects on astrocytes compared with nanoflakes at the same sublethal exposure to different concentrations (31.25, 62.5, and 125 μg/mL) for 72 h.

Several studies were conducted to evaluate the hepatorenal toxic potential of AL_2O_3 NPs in animal models. Kumari et al. [13] found that Al_2O_3 had a hepatotoxic effect, with greater toxicity for smaller sizes compared to larger ones. Yousef et al., [8] showed that oral treatment with AL and ZN oxide nanoparticles caused hepato-renal toxicity with the development of focal necrosis in the liver and congestion of the central vein, degeneration in hepatocytes, on the kidney level, degeneration and cellular infiltration in renal tubules, vacuolation and distortion in renal corpuscles and shrinkage of their capillaries. Alghriany et al., [14] revealed that Al_2O_3 and Al_2O_3 NPs induced hepatocyte apoptosis decreased antitrypsin and IgG in the serum, increased total white blood cells, and excessive inflammatory activation, in addition to induction of hepatic fibrosis by increasing amounts of pro-fibro genic chemicals, such as the transforming growth factor-β1 in mouse liver responsible for increase activation of hepatic stellate cells.

The present study has focused on evaluating the hepatotoxic potential of different shapes of aluminum oxide nanoparticles-AL_2O_3 NPs (spheres and rods) in rats via estimation of oxidative hepatic markers, hepatic histopathology, and selective characterization of SIRT-1 and AMPK hepatic expression by immunohistochemistry.

Material and Methods

Aluminum oxide nanoparticle synthesis

Aluminum oxide nanoparticles with a spherical shape were synthesized using a water-in-oil microemulsion technique [15] . Briefly, an aqueous solution of 1 M $AlCl_3$ was added dropwise to the cyclohexane and Triton X-100 mixture (70:30 w/w) while stirring. Ammonia solution was added to hydrolyze $AlCl_3$ until the reaction system pH reached ~9.5 to produce Al_2O_3 precursors. Next, ethanol (95%) was added to the mixture and stirred for 30 minutes until evaporation. The NPs were pelleted by centrifugation at 12,000 rpm, followed by washing with ethanol and water three times each.

Aluminum oxide nanorods were synthesized as previously described [16]. Briefly, ethylene diamine solution was added dropwise to the aqueous solution of aluminum nitrate while stirring until the pH reached ~5. After stirring for 30 minutes, the reaction mixture was incubated at 180°C in an oven for 72 hr. Afterward, the mixture was immediately cooled and centrifuged at 12,000 rpm, then washed with ethanol and water three times each.

Al_2O_3 NPs characterization

Unhydrated NP diameter was determined using a high-resolution transmission electron microscope (JEOL, JEM-2100) at an accelerating voltage of 200 kV. Average diameters of 500 particles were determined from TEM images (n=3) using image analysis software (ImageJ, National Institutes of Health, version 1.5a, ImageJ.nih.gov). Zeta potential analyses were performed to determine the surface charge of hydrated NPs [Malvern, Malvern, UK (Zeta sizer Nano ZS90)[17].

Animals and ethics statement

Thirty-five mature male Wister rats, weighing 150 gm. were obtained from the animal house of VACSERA and housed in a plastic cage. The experimental animals had access ad libitum to water and a balanced commercial pelleted diet. Animals were maintained in a controlled atmosphere, a temperature of 25 ± 5 °C and 50–70% humidity, a light/ dark cycle of 12 hr. /12 hr.

The experimental procedures were approved by the Ethical Committee of the Institutional Animal

Care and Use Committee (IACUC), Cairo University, Egypt (approval number: CU II F 13 22).

Experimental design

Thirty-five rats were divided into five groups 7 rats per group, control untreated rats received 0.5 ml of distilled water, Al_2O_3 NPs treated groups with two different shapes (spheres and rods) at doses of 20 mg and 40 mg/kg B.W. of body weight for the two shapes, treatment was conducted orally using gastric intubation once daily for 2 months, at the end of an experimental period blood collection was performed then rats were euthanized and livers were collected for further processing.

Determination of Serum Hepatic Enzymes

Serum samples were collected from different experimental groups of rats following the 60-day exposure period. Estimation of alanine aminotransferase (ALT) and alkaline phosphatase (ALP) using spectrophotometric kits provided by Bio Diagnostic Kits, Giza, Egypt, and according to Reitman [18].

Determination of Total Antioxidant Capacity (TAC)

The liver tissue homogenate was used for the estimation of TAC content using spectrophotometric kits provided by Bio Diagnostic Kits, Giza, Egypt.[19]

Histopathological &histochemical evaluations

Liver specimens were routinely fixed in neutral buffered formalin and then processed according to Suvarna et al. [20]. Liver histological slide sections were examined in an Olympus BX43 light microscope and captured using an Olympus DP27 camera linked to cellSens dimensions software (Olympus). Scoring of liver lesions was performed into four grades as follows: 1(minimal),2 (mild), 3(moderate), and 4 (severe).

In addition, the selected section was stained by Masson`s Trichrome (MTC) for characterization of collagen deposition

Immunohistochemical evaluation of SIRT-1 &AMPK hepatic expressions

Histological hepatic sections were immunoassayed using an immunohistochemistry detection kit against SIRT1, and AMPK (ab110304), bs-22269R, Santa Cruz Biotechnology, Inc., Heidelberg, Germany, dilution of 1:200). Sections were deparaffinized in xylene (3 changes of each for 5 min), then hydrated in a decreasing gradient of alcohol for 5 min each. Endogenous peroxidase was blocked by immersing sections with 3% hydrogen peroxide in methanol, followed by heat-induced antigen retrieval in 10 mM citrate buffer with 0.05% Tween-20 (pH 6.0). After cooling, Sections were treated with primary antibodies (1:200 dilution) in blocking solution for 2 h 30 min at room temperature, followed by horse radish peroxidase (HRP) labeled secondary antibody for 30 minutes at room temperature (anti-Rabbit HRP-DAB Micro-polymer IHC Kit ab236466, Abcam, Cambridge, UK, 1:200). Staining was visualized by covering the sections in buffer containing 3′-3′ diaminobenzidine (DAB) ((Pierce™ DAB Substrate Kit (34002), Thermo Scientific, Inc., Rockford, IL, USA) was used to develop the reaction for 5 min, counterstained by hematoxylin counterstaining. After dehydration, sections were mounted and images were captured with cell Sens Dimension software, Olympus, Tokyo, Japan. Negative control slides were prepared by removing the primary antibody incubation step.

Statistical analysis

All statistical analyses in GraphPad Prism version 9.3.1 (GraphPad Software, La Jolla, CA) were performed using one-way and two-way analysis of variance (ANOVA) with Tukey multiple comparison test. p values ≤ 0.05 were considered statistically significant.

Results

Synthesis and Characterization of Al_2O_3 NPs

The morphology of Al_2O_3 NPs is depicted in Fig.1A. Al_2O_3 NPs exhibit a spherical morphology with an average diameter of 34.5 ± 5.2 nm, while (Fig.1B) a rod-shaped morphology with an average diameter of 21.4 ± 4.7 nm and an average length of 166.8 ± 17.4 nm. The zeta potentials of Al_2O_3 NPs, sphere and rod shapes, are measured to be -17.2 ± 0.4 mV and -13.4 ± 0.3 mV, respectively.

Biochemical Analysis

The serum ALP and ALT levels were significantly increased in higher doses of the intoxicated groups and nanospheres, more than nano rods Al_2O_3 NPs, compared with lower doses and the control group. (Fig.2 A, B).

Reduction of TAC in the liver

A dose-dependent reduction in the total antioxidant activity level in liver tissue was detected in rats that received nano spheres rather than nano rods (Fig.3).

Histopathological findings

Microscopic examination of the control group revealed normal hepato-parenchymal architecture. The microscopic examination of the intoxicated group revealed various hepatic alterations, and the lesion score was summarized in Fig.4. The lesion severity was dose and shape-dependent. The microscopic examination of nanospheres (NPS) revealed hepatocellular apoptosis (Fig.5A), and focal random macrovesicular steatosis was evident (Fig.5B). The portal triads exhibited microangiopathy characterized by hyaline thickening

of portal vasculature that involved both hepatic arterioles and portal venules associated with endothelial swelling (Fig. 5C&D), portal mononuclear cell aggregation (C), minimal portal fibroplasia, and oval cell proliferation (G&H). The hepatic lesions were more pronounced with higher doses of NPS (Fig. 5E, F, G& H) . Severe portal fibrosis, bile duct hyperplasia, and marked oval cell proliferation were encountered in this group, in addition to the severe grade of the previously described hepatic lesions in the lower dose-intoxicated group.

Concerning the hepatic lesions in the nanorods (NRS) intoxicated group, the lower dose (Fig. 5I&J) exhibited minimal hepatocellular apoptosis, and microangiopathy was more like the NPS intoxicated group of similar doses, but involving individual portal triads.

The portal fibroplasia was confirmed by histochemical characterization of portal triads stained by Masson`s Trichrome (MTC) for characterization of collagen deposition compared with the control one (Fig. 6A-c).

The hepatic expressions of SIRT-1 &AMPK

The immunohistochemical analysis of hepatic expressions for SIRT1 and AMPK revealed variation in immunoreactivity between different intoxicated groups compared with the control one. The control group showed moderate cytoplasmic expression for both SIRT1 and AMPK, while there was a reduction and downregulation of expression for SIRT1 and AMPK in all intoxicated groups.The downregulation rate was dose-dependent and more pronounced in NPS than in NRS (Fig.7).

Discussion

Aluminum oxide nanoparticles (Al_2O_3 NPs) have been recently used for medical purposes. The shape-dependent toxicity of nanoparticles was previously discussed in some research works. Since the liver is the primary target organ for orally induced toxicity, the present study is conducted to evaluate the shape-dependent hepatotoxicity of Al_2O_3 NPs after 60 days of oral treatment of rats. There are two shapes of Al_2O_3 NPs used in the present study, nanospheres (NPs) and nanorods (NRs), with doses of 20 and 40 mg/kg b.w. The present study revealed that NPs have relatively larger diameters (34.5 ± 5.2 nm) compared with nanorods (21.4 ± 4.7 nm) via TEM characterization, with high zeta potential for NPs relative to NRs. The data related to hepatic oxidative stress markers revealed that Al_2O_3 NPs induced exaggerated oxidative stress on the liver with higher adverse effects in NPs than NRs and increased with advancing dose; these findings correlated with both biochemical elevations of hepatic enzymes and hepatocellular reactions that included both necrotic and inflammatory reactions in the liver parenchyma. These results clarified that although the NPs are larger in diameter than NRs, which exhibit more toxic action, these results confirmed that not only does the size of nanoparticles determine their toxicity, but also the shape is considered as an additional factor and should be considered. Prabhakar et al. [21] found that acute oral intoxication of Wistar rats with 30 nm and 40 nm of Al_2O_3 nanoparticles had the potential to induce oxidative stress after acute oral treatment with high doses of Al_2O_3 nanoparticles (30 nm and 40 nm) and bulk Al_2O_3 in Wistar rats. Another study confirmed that Al_2O_3 NPCs induced damage in various organs (liver, kidney, brain) of mice after exposure to different doses for 5 days, and they correlated this damage to increased AL accumulation in these organs [22]. Previous research clarified the role of Al_2O_3 NPCs in the induction of oxidative tissue damage and activation of proapoptotic genes in the liver [14,23].

The current work proved the potential of Al_2O_3 NPCs to induce microangiopathy of hepatic vasculatures, the lesion characterized histopathologically by marked thickening and hyalinization of hepatic arterioles, and portal venules associated with a variant degree of portal cholangiofibrosis in a dose and shape-dependent manner. In addition to the inflammatory, degenerative, and necrotic reactions that were evident in intoxicated groups compared with the control one. These findings are in correlation with the downregulation of expression for AMPK and SIRT-1. Previous studies clarified the vital role of SIRT 1 in liver metabolism, as it is considered a key metabolic sensor in the liver. the function of SIRT1 is initiated by the breakdown of the nicotinamide ribosyl bond of NAD+ with translocation of the acetyl group from the substrate's lysine side chain to NAD+, resulting in generating nicotinamide, 2'-O-acetyl-ADP-ribose, and a deacetylated substrate [24,25], this indicated that the activity of SIRT1 can be initiated by increasing the cellular NAD+ levels and suppressed by increased nicotinamide levels [26]. The deficiency of SIRT1 in hepatocytes can impair fat metabolism, resulting in hepatic steatosis [27].

Recent research confirmed that deficiency of SIRT 1 induced fatty liver irrespective of dietary fat content, and its disruption induced hepatic steatosis, initiating advanced hepatic disorders [28].

Liver damage is promoted by oxidative stress on hepatocytes, resulting in mitochondrial dysfunction and apoptosis [29]. The level of cellular reactive oxygen species (ROS) and antioxidant capacity determines the magnitude of cellular stress [30]. The regulatory effect of SIRT1 on oxidative stress has been reported in various studies, as SIRT1 increased the transcriptional activity of FOXOs and PGC-1α on antioxidant enzyme genes. Blokker et al. [31] found

that control of SIRT1 expression is crucial in protecting the liver from cholestasis-inducing liver damage. It was found that the hepatic expression of SIRT1 regulated anti-apoptotic Bcl-2/XIAP proteins [32] . The cytoplasmic localization of SIRT1 was considered a proapoptotic factor [33], while its nuclear localization functioned as an anti-apoptotic factor [34,35].

SIRT1 expression in normal liver tissue has been reported to be faint to moderate [36]. However, its depletion in the liver of mice has been shown to promote hepatic steatosis, inflammation, and fibrosis following ethanol exposure [37], highlighting its protective role in maintaining liver homeostasis. This protective effect is, in part, attributed to SIRT1's ability to reduce reactive oxygen species (ROS) levels in various tissues, including the liver. Mechanistically, SIRT1 regulates oxidative stress by deacetylating transcription factors such as FOXOs and PGC-1α, which enhances their transcriptional activity and promotes the expression of antioxidant enzymes [38–40]. Consistently, increased expression of SIRT1 has been shown to upregulate antioxidant gene expression, thereby mitigating the harmful effects of oxidative stress on hepatic tissue [41,42].

The role of SIRT1 in inflammation was previously confirmed; it was found that SIRT1 has the potential to decrease hepatic inflammation via deacetylating NF-Kb [28] and the transgenic mice with overexpressed SIRT1 have lower levels of inflammatory cytokines via downregulation of NF-κB.[37,43].

Downregulation of SIRT1 has been observed in vascular injury and microangiopathy among diabetic patients, suggesting its involvement in the pathogenesis of diabetic vascular complications [44]. Given the crucial role of AMPK signaling in ameliorating lipid metabolism disorders and reducing liver injury, recent studies have investigated the interaction between AMPK and SIRT1. Fang et al. [45] and Long et al. [46] demonstrated that AMPK enhances SIRT1 activity by increasing the intracellular AMP/ATP ratio, thereby promoting metabolic homeostasis. Moreover, SIRT1 has been shown to induce the cytoplasmic translocation of LKB1, which subsequently activates AMPK, forming a positive feedback loop that regulates fat metabolism. In addition, AMPK agonists contribute to the modulation of inflammation and oxidative stress in hepatocytes, further supporting the therapeutic relevance of this pathway [47]

Conclusion

The present study confirmed the hepatotoxic potential of aluminum nanoparticles, highlighting the potential for hepatotoxicity through the induction of oxidative stress and the downregulation of AMPK and SIRT-1, accompanied by hepatic microangiopathy, necrosis, and inflammation

Acknowledgments

Not applicable.

Funding statement

This study didn't receive any funding support

Declaration of Conflict of Interest

The authors declare that there is no conflict of interest.

Ethical of approval

The experimental procedures were approved by the Ethical Committee of the Institutional Animal Care and Use Committee (IACUC), Cairo University, Egypt (approval number: CU II F 13 22).

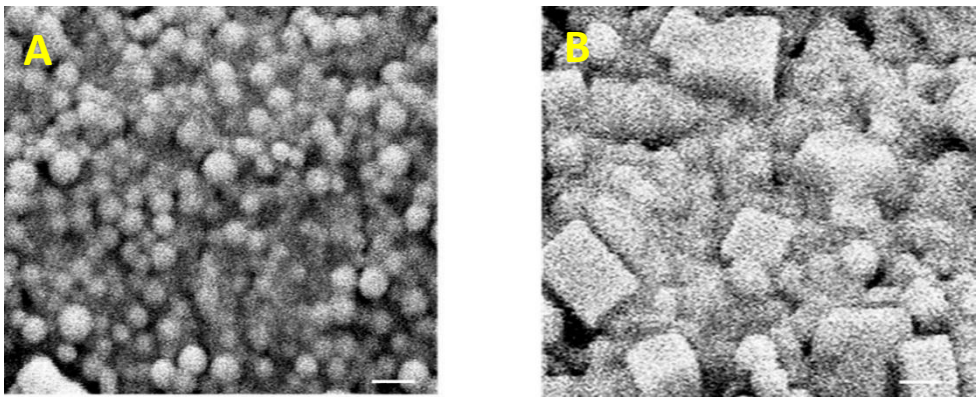

Fig. 1. SEM images of (A) Al_2O_3 NPs, sphere shape and (B) Al_2O_3 NPs, rod shape. The scale bar represents 50 nm

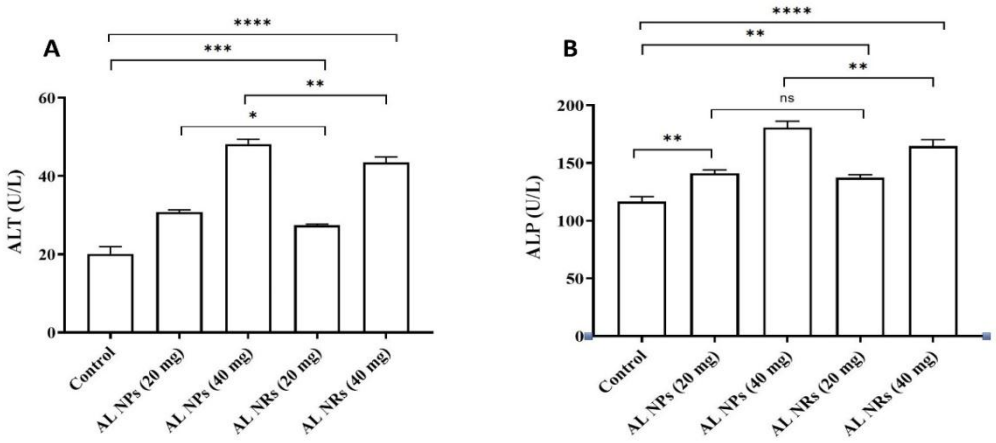

Fig. 2. Effect of Al_2O_3 nanospheres (NPs) and rods(NRs) on serum ALT (A) and ALP (B) levels in Male Wistar rats, Data represent the mean ± standard deviation (n=5). Statistical differences between groups are denoted by (*p ≤ 0.05, **p ≤ 0.01, ***p ≤ 0.001, and ****p ≤ 0.0001).

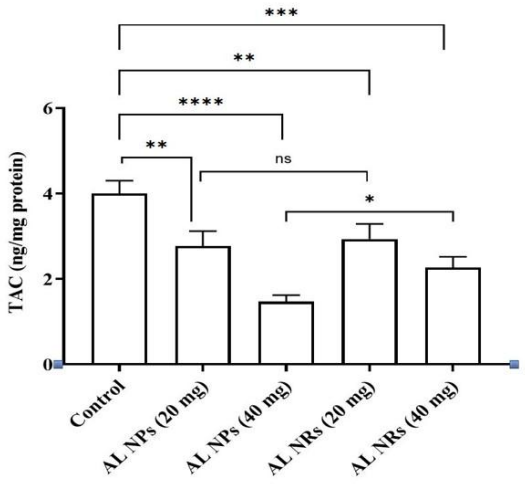

Fig. 3. Effect of Al_2O_3 nanospheres (NPs) and rods (NRs) on TAC in liver tissue w Data represent the mean ± standard deviation (n=5). Statistical differences between groups are denoted by (*p ≤ 0.05, **p ≤ 0.01, ***p ≤ 0.001, and ****p ≤ 0.0001).

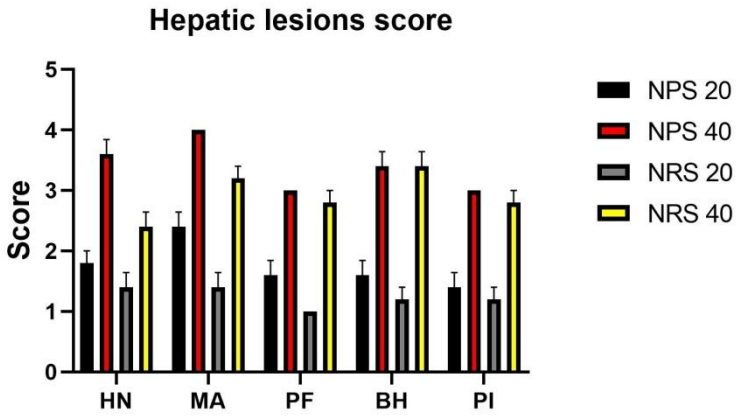

Fig. 4. Qualitative analysis graph for hepatic lesions as follows: 1 (minimal), 2(mild), 3(moderate), and 4 (severe).HN: hepatocellular necrosis, MA: Microangiopathy, PF: portal fibrosis, BH: biliary hyperplasia, PI: portal inflammatory cells infiltration.

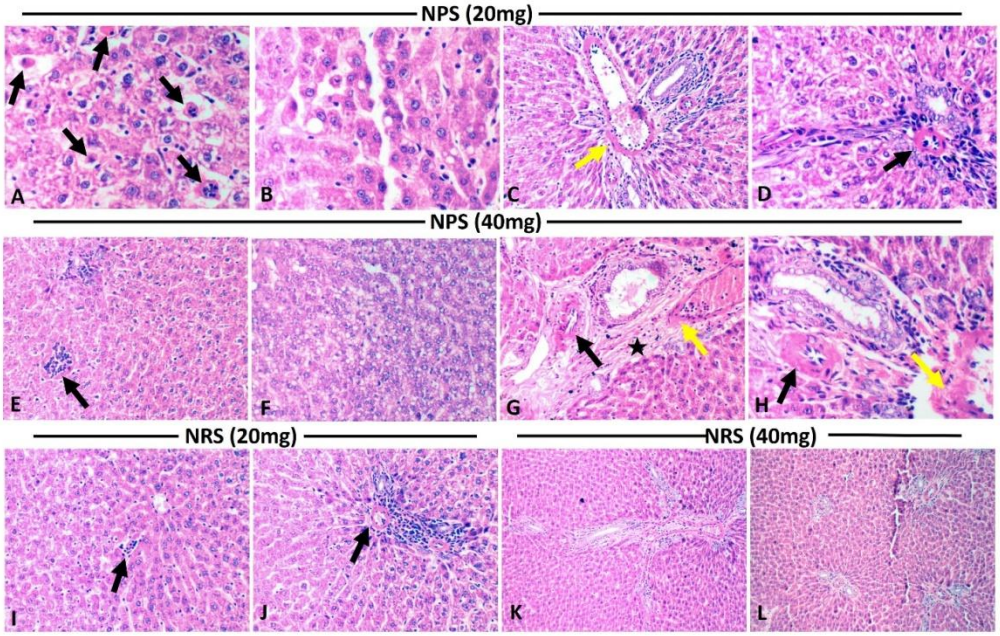

Fig. 5. Photomicrograph of the liver in different Al_2O_3 NPCs intoxicated groups (H&E):A-D liver of rat treated with 20mg of nanosphere (NPS) showing: (A)individual cell necrosis with karyopyknosis & karyorrhexis of hepatocellular nuclei (black arrows) (Magnification X400).(B)hepatocellular micro and macrovesicular steatosis of individual hepatocytes associated with single cell necrosis (Magnification X400).(C) thickening of portal b.v (yellow arrow) with few portal mononuclear cell infiltration (Magnification X200).(D) microangiopathy of hepatic arteriole, note the dense hyalinization and thickening of vascular wall (black arrow) associated with minimal biliary hyperplasia and scant portal fibrosis (Magnification X200). E-H liver of rat treated with 40mg of nanosphere (NPS) showing: (E) multifocal hepatocellular necrosis infiltrated by mononuclear cells (black arrow) (Magnification X200). (F)diffuse hepatocellular steatosis (Magnification X400). (G) Severe thickening of the portal venule (yellow arrow) and hepatic arteriole of the portal area with vacuolation of the arteriolar wall (black arrow) associated with bile duct hyperplasia and marked portal fibrosis (asterisk) (Magnification X200). (H) Severe hyalinization and thickening of the hepatic (black arrow) and portal vascular wall (yellow arrow) (Magnification X400). I-J liver of rat treated with 20mg of nanorods (NRS) showing: (I) individual hepatocellular necrosis with scarce sinusoidal lymphocytic infiltration (black arrow)(Magnification X200). (J) moderate thickening of the capillary vascular wall (black arrow) of a small portal area with portal mononuclear cell infiltration (Magnification X200). K-L liver of rat treated with 40 mg of nanorods (NRS) showing: (K) portal fibrosis of medium-sized portal area associated with few mononuclear cells infiltration and thickened portal wall vasculatures Magnification X100). (L) Marked distention of multiple small portal areas by fibrosis with thickening of the small vascular wall (Magnification X100).

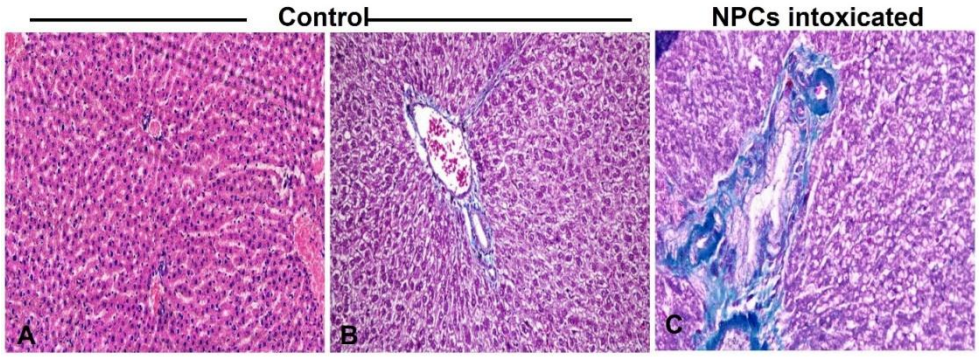

Fig. 6. Photomicrograph of the liver in control untreated (A-B) and Al_2O_3 NPCs intoxicated groups (C); (A) control rat liver showing the normal histological structure and size of the small portal area and normal thickness of the vascular wall (Magnification,100X, H&E). (B) control rat liver with normal collagen density in the portal area (Magnification,100X, MTC).(C) liver from rat intoxicated with Al_2O_3,40 mg, NPS showing increase collagen density in thickened vascular walls and moderate collagen deposition in portal area(Magnification,200X, MTC).

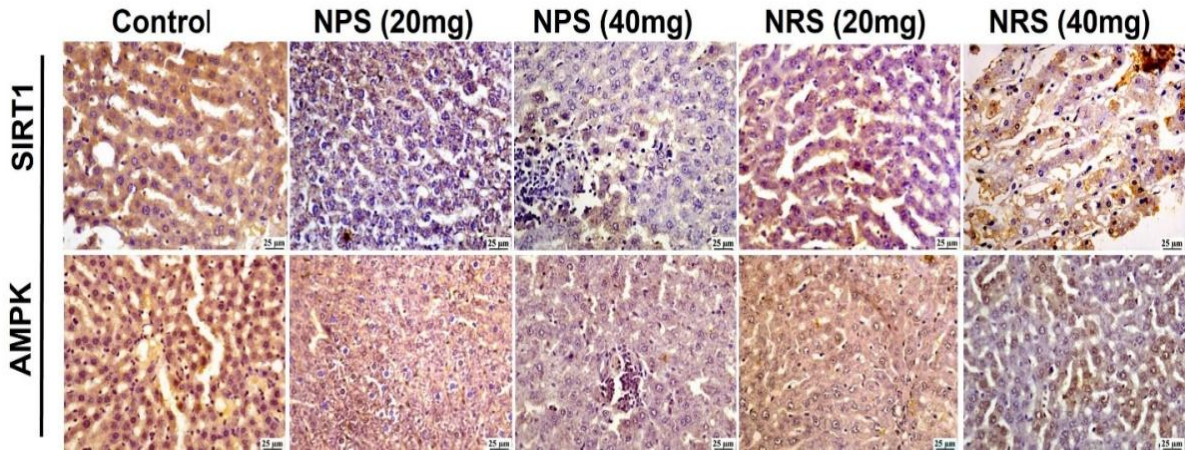

Fig. 7. Photomicrograph of immunohistochemically stained section for AMPK &SIRT1 expression in different experimental groups.

References

1. Zuo, J., Qin, Y., Zhao, Z., Xing, L., Liu, T., Wang, S. and Liu, W. Preparation, properties and antibacterial applications of medical nano-metals and their oxides: a review]. Sheng Wu Gong Cheng Xue Bao . *Chinese Journal of Biotechnology*, **39**(4), 1462–1476 (2023). https://doi.org/10.13345/J.CJB.220536.
2. Zain, H. Y., Sunishtha, S. Y., Sidra, A., Muhammad, B. Aqsa, S. and Mohsi, N K., Applications of nanotechnology in biological systems and medicine,Editor(s): Adil Denizli, Tuan Anh Nguyen, Mariappan Rajan, Mohammad Feroz Alam, Khaliqur Rahman, In Micro and Nano Technologies, Nanotechnology for Hematology, Blood Transfusion, and Artificial Blood, *Elsevier*, 215-235(2022). https://doi.org/10.1016/B978-0-12-823971-1.00019-2.
3. Wang, N., Wei, C., Zhang, Z., Liu, T. and Wang, T. Aluminum nanoparticles acting as a pulmonary vaccine adjuvant-delivery system (VADS) able to safely elicit robust systemic and mucosal immunity. *Journal of Inorganic and Organometallic Polymers and Materials*, **30**, 4203-4217(2020).
4. Lu, Y. and Liu, G. Nano alum: A new solution to the new challenge. *Human Vaccines & Immunotherapeutics*, **18**(5), 2060667(2022).
5. Hassanpour, P., Panahi, Y., Ebrahimi-Kalan, A., Akbarzadeh, A., Davaran, S., Nasibova, A.N., Khalilov, R. and Kavetskyy, T. Biomedical applications of aluminium oxide nanoparticles. *Micro Nano Lett.*, **13**, 1227-1231 (2018).. https://doi.org/10.1049/mnl.2018.5070
6. Lun, D. and Xu, K. Recent progress in gas sensor based on nanomaterials. *Micromachines*, **13**(6), 919. (2022).
7. Wu, Z., Du, Y., Xue, H., Wu, Y. and Zhou, B. Aluminum induces neurodegeneration and its toxicity arises from increased iron accumulation and reactive oxygen species (ROS) production. *Neurobiology of Aging*, **33**(1), 199-e1. (2012).
8. Yousef, M. I., Mutar, T. F. and Kamel, M. A. E. N. Hepato-renal toxicity of oral sub-chronic exposure to aluminum oxide and/or zinc oxide nanoparticles in rats. *Toxicology Reports*, **6**, 336-346(2019).
9. Willhite, C.C., Karyakina, N.A., Yokel, R.A., Yenugadhati, N., Wisniewski, T.M., Arnold, I.M., Momoli, F. and Krewski, D. Systematic review of potential health risks posed by pharmaceutical, occupational and consumer exposures to metallic and nanoscale aluminum, aluminum oxides, aluminum hydroxide and its soluble salts. *Crit. Rev. Toxicol.*, **44** (Suppl.4), 1-80 (2014). doi: 10.3109/10408444.2014.934439. PMID: 25233067;
10. Brill-Karniely, Y., Schwob, O. and Benny, O. The aspect ratio effect on the cytotoxicity of inert nano-particles flips depending on particle thickness, and is one of the reasons for the literature inconsistency. *Nanoscale Advances*, **4**(24), 5257-5269 (2022).
11. Park, E. J., Lee, G. H., Yoon, C., Jeong, U., Kim, Y., Cho, M. H. and Kim, D. W. Biodistribution and toxicity of spherical aluminum oxide nanoparticles. *Journal of Applied Toxicology*, **36**(3), 424-433(2016).
12. Dong, L., Tang, S., Deng, F., Gong, Y., Zhao, K., Zhou, J., Liang, D., Fang, J., Hecker, M., Giesy, J.P., Bai, X. and Zhang, H. Shape-dependent toxicity of alumina nanoparticles in rat astrocytes. *Sci. Total Environ.*, **690**, 158-166(2019). doi: 10.1016/j.scitotenv.2019.06.532. Epub 2019 Jul 2. PMID: 31284190.
13. Kumari, S. A., Madhusudhanachary, P., Patlolla, A. K. and Tchounwou, P. B. Hepatotoxicity and ultra structural changes in Wistar rats treated with Al_2O_3 nanomaterials. *Trends In Cell & Molecular Biology*; **11**, 77 (2016).
14. Alghriany, A. A., Omar, H. E. D. M., Mahmoud, A. M. and Atia, M. M. Assessment of the toxicity of aluminum oxide and its nanoparticles in the bone marrow and liver of Male mice: Ameliorative efficacy of curcumin nanoparticles. *ACS Omega*,. **7**(16), 13841-13852(2022).

15. Sun, B., Ji, Z., Liao, Y.P., Wang, M., Wang, X., Dong, J., Chang, C.H., Li, R., Zhang, H., Nel, A.E. and Xia, T. Engineering an effective immune adjuvant by designed control of shape and crystallinity of aluminum oxyhydroxide nanoparticles. *ACS Nano*., **7**(12), 10834-10849(2013). doi: 10.1021/nn404211j. Epub 2013 Dec 2. PMID: 24261790; PMCID: PMC3899397.

16. Mahmoud, M. Y., Steinbach-Rankins, J. M. and Demuth, D. R. Functional assessment of peptide-modified PLGA nanoparticles against oral biofilms in a murine model of periodontitis. *Journal of Controlled Release*, **297**, 3-13(2019).

17. Guglielmotto, M., Aragno, M., Autelli, R., Giliberto, L., Novo, E., Colombatto, S., Danni, O., Parola, M., Smith, M.A., Perry, G., Tamagno, E. and Tabaton, M. The up-regulation of BACE1 mediated by hypoxia and ischemic injury: role of oxidative stress and HIF1alpha. *J. Neurochem.*, **108**(4), 1045-1056 (2009). doi: 10.1111/j.1471-4159.2008.05858.x. PMID: 19196431

18. Reitman, F.S., A colorimetric method for the determination of serum glutamic oxalacetic and glutamic pyruvic transaminases. *Am. J. Clin. Pathol.*, **28**(1), 56–63(1957). doi: 10.1093/ajcp/28.1.56. PMID: 13458125

19. Benzie, I.F. and Strain, J.J., Ferric reducing/antioxidant power assay: direct measure of total antioxidant activity of biological fluids and modified version for simultaneous measurement of total antioxidant power and ascorbic acid concentration. InMethods in enzymology 1999 Jan 1 (Vol. 299, pp. 15-27). Academic press.

20. Suvarna, S., Kim, Christopher, L. and John, D., Bancroft :Bancroft's Theory and Practice of Histological Techniques, 8th edition, Elsevier, 2019, ISBN 070206887X, 9780702068874., 536 pages https://doi.org/10.1016/C2015-0-00143-5

21. Prabhakar, P.V., Reddy, U.A., Singh, S.P., Balasubramanyam, A., Rahman, M.F., Indu Kumari, S., Agawane, S.B., Murty, U.S., Grover, P. and Mahboob, M. Oxidative stress induced by aluminum oxide nanomaterials after acute oral treatment in Wistar rats. *J. Appl. Toxicol.*, **32**(6), 436-445(2012). doi: 10.1002/jat.1775.

22. De A, Ghosh, S., Chakrabarti, M., Ghosh, I., Banerjee, R. and Mukherjee, A., Effect of low-dose exposure of aluminium oxide nanoparticles in Swiss albino mice: Histopathological changes and oxidative damage. *Toxicology and Industrial Health.* **36**(8), 567-579(2020). doi:10.1177/0748233720936828.

23. Karami, E., Goodarzi, Z., Shahtaheri, S. J., Kiani, M., Faridan, M. and Ghazi-Khansari, M. The aqueous extract of Artemisia Absinthium L. stimulates HO-1/MT-1/Cyp450 signaling pathway via oxidative stress regulation induced by aluminium oxide nanoparticles (α and γ) animal model. *BMC Complementary Medicine and Therapies*, **23**(1), 310 (2023).

24. Sinclair, D.A. and Guarente, L., Extrachromosomal rDNA circles-a cause of aging in yeast. *Cell*, **91**,1033-1042 (1997).

25. Xie, J., Zhang, X.M. and Zhang, L., Negative regulation of inflammation by SIRT1. *Pharmacol. Res.*, **67**, 60-67(2013).

26. Rajamohan SB, Pillai VB, Gupta M, Sundaresan NR, Birukov KG, Samant S, Hottiger MO, Gupta MP.. SIRT1 promotes cell survival under stress by deacetylation-dependent deactivation of poly(ADP-ribose) polymerase 1. *Mol. Cell Biol.*, **29**,4116-129. (2009).

27. Purushotham, A., Schug, T.T., Xu, Q., Surapureddi, S., Guo, X. and Li, X. Hepatocyte-specific deletion of SIRT1 alters fatty acid metabolism and results in hepatic steatosis and inflammation. *Cell Metab.*, **9**,327–338(2009).

28. Ding, R.B., Bao, J. and Deng, C.X., Emerging roles of SIRT1 in fatty liver diseases. *International Journal of Biological Sciences*, **13**(7), 852-867 (2017). https://doi.org/10.7150/ijbs.19370.

29. Purohit, V., Gao, B. and Song, B.J., Molecular mechanisms of alcoholic fatty liver. *Alcohol Clin. Exp. Res.*, **33,**191-205(2009).

30. Ji, LL. Antioxidants and oxidative stress in exercise. Proc.Soc. Exp. Biol. Med., **222**, 283-292. (1999).

31. Blokker, B. A., Maijo, M., Echeandia, M., Galduroz, M., Patterson, A. M., Ten, A., Philo, M., Schungel, R., Gutierrez-de Juan, V., Halilbasic, E., Fuchs, C., Le Gall, G., Milkiewicz, M., Milkiewicz, P., Banales, J. M., Rushbrook, S. M., Mato, J. M., Trauner, M., Müller, M., Martínez-Chantar, M. L. and Beraza, N. Fine-Tuning of Sirtuin 1 Expression Is Essential to Protect the Liver From Cholestatic Liver Disease. *Hepatology (Baltimore, Md.)*. **69**(2), 699–716(2019). https://doi.org/10.1002/hep.30275.

32. Kentaro Kadono, Hidenobu Kojima1,4, Siyuan Yao1 , Shoichi Kageyama1,2, Kojiro Nakamura1,2, Hirofumi Hirao1 , Takahiro Ito1 , Kenneth J. Dery1 , Douglas G. Farmer1 , Fady M. Kaldas1 , Xiaoling Li 3 and Jerzy W. Kupiec-Weglinski. SIRT1 regulates hepatocyte programmed cell death via GSDME - IL18 axis in human and mouse liver transplantation. *Cell Death Dis.*, **14**, 762 (2023). https://doi.org/10.1038/s41419-023-06221-0

33. Jin, Q., Yan, T., Ge, X., Sun, C., Shi, X. and Zhai, Q.Cytoplasm-localized SIRT1 enhances apoptosis. *J. Cell. Physiol.*, **213**, 88–97(2007). doi: 10.1002/jcp.21091.

34. Hisahara, S., Chiba, S., Matsumoto, H., Tanno, M., Yagi, H., Shimohama, S., Sato, M. and Horio, Y. Histone deacetylase SIRT1 modulates neuronal differentiation by its nuclear translocation. Proc. *Natl. Acad. Sci., U.S.A.*, **105**,5599–15604(2008). doi: 10.1073/pnas.0800612105.

35. Tong, C., Morrison, A., Mattison, S., Qian, S., Bryniarski, M., Rankin, B., Wang, J., Thomas, D.P. and Li, J.Impaired SIRT1 nucleocytoplasmic shuttling in the senescent heart during ischemic stress. *FASEB J.*, **27**, 4332–4342 (2013). doi: 10.1096/fj.12-216473.

36. Redha A., Dominika, T., Samar, Z., Yasser, A. and Seishi, N., Differential SIRT1 Expression in Hepatocellular Carcinomas and Cholangiocarcinoma of the Liver. *Ann. Clin. Lab. Sci.,* 45(1), 3-9(2015).

37. Yin H, Hu M, Liang X, Ajmo JM, Li X, Bataller R, Odena G, Stevens SM Jr, You M.Deletion of SIRT1 from hepatocytes in mice disrupts lipin-1 signaling and aggravates alcoholic fatty liver. *Gastroenterology*, **146**, 801-811(2014).

38. Rodgers, J.T., Lerin, C., Haas, W., Gygi, S.P., Spiegelman, B.M. and Puigserver, P. Nutrient control of glucose homeostasis through a complex of PGC-1alpha and SIRT1. *Nature*, **434**,113-118(2005).

39. Brunet A, Sweeney LB, Sturgill JF, Chua KF, Greer PL, Lin Y, Tran H, Ross SE, Mostoslavsky R, Cohen HY, Hu LS, Cheng HL, Jedrychowski MP, Gygi SP, Sinclair DA, Alt FW, Greenberg ME. Stress-dependent regulation of FOXO transcription factors by the SIRT1 deacetylase. Science, 303, 2011-2015 (2004).

40. Li, M., Guo, K., Vanella, L., Taketani, S., Adachi, Y., Ikehara S. Stem cell transplantation upregulates Sirt1 and antioxidant expression, ameliorating fatty liver in type 2 diabetic mice. Int. J. Biol. Sci., 11,472-81(2015).

41. Feige, J.N., Lagouge, M., Canto, C., Strehle, A., Houten, S.M., Milne, J.C. et al. Specific SIRT1 activation mimics low energy levels and protects against diet-induced metabolic disorders by enhancing fat oxidation. Cell Metabolism, 8,347-358 (2008).

42. Canto, C., Houtkooper, R.H., Pirinen, E., Youn, D.Y., Oosterveer, M.H., Cen, Y. et al. The NAD(+) precursor nicotinamide ribosi,de enhances oxidative metabolism and protects against high-fat diet-induced obesity. Cell Metabolism, 15,838-847 (2012).

43. Nakamura, K., Kageyama, S., Ke, B., Fujii, T., Sosa, R.A., Reed, E.F., et al. Sirtuin 1 attenuates inflammation and hepatocellular damage in liver transplant ischemia/Reperfusion: From mouse to human. Liver Transpl., 23,1282–1293(2017).

44. Qi, J., Tongtong, L., Fang, M., Tongfei, F., Liping, Y., Huimin, M., Yuyang, W., Liang, P., Ping, L. and Yongli, Z., Roles of Sirt1 and its modulators in diabetic microangiopathy: A review, International Journal of Biological Macromolecules, 264, Part 2, (2024).130761,ISSN 0141-8130.

45. Fang, C., Pan, J., Qu, N., Lei, Y., Han, J., Zhang, J., and Han, D. The AMPK pathway in fatty liver disease. Frontiers in Physiology, 13, 970292(2022). https://doi.org/10.3389/fphys.2022.970292.

46. Long, J.-K., Dai, W., Zheng, Y.-W. and Zhao, S.-P. MiR-122 promotes hepatic lipogenesis via inhibiting the LKB1/AMPK pathway by targeting Sirt1 in non-alcoholic fatty liver disease. Mol. Med., 25 (1), 26. (]2019).10.1186/s10020-019-0085-2

47. Lan, F., Cacicedo, J. M., Ruderman, N. and Ido, Y. SIRT1 modulation of the acetylation status, cytosolic localization, and activity of LKB1. Possible role in AMP-activated protein kinase activation. J. Biol. Chem., 283 (41), 27628–27635 (2008). 10.1074/jbc.M805711200

اختلال تنظيم التعبير عن AMPK و Sirt-1 في الكبد يتسبب في إصابة الكبد واعتلال الأوعية الدقيقة الناجم عن جسيمات أكسيد الألومنيوم النانوية في الفئران مع التركيز بشكل خاص على السمية الكبدية المعتمدة على الشكل

اسراء محمود حجازى[1] ، محمد محمود يحيى[2] ، فاتن فتحى محمد[1,3] و مجدى محمد المهدى[1]

[1] قسم الباثولوجيا، كلية الطب البيطري، جامعة القاهرة، مصر.

[2] قسم السموم والطب الشرعى ، كلية الطب البيطري، جامعة القاهرة، مصر.

[3]قسم الباثولوجيا، كلية الطب البيطري، جامعة الملك فيصل، المملكة العربية السعودية.

الملخص

تُستخدم جسيمات أكسيد الألومنيوم النانوية (Al2O3) على نطاق واسع في أغراض طبية متنوعة، بما في ذلك توصيل الأدوية؛ لذا، يُعدّ تقييم سلامة سُميتها أمرًا بالغ الأهمية. هدفت هذه الدراسة إلى تقييم احتمالية سمية جسيمات أكسيد الألومنيوم النانوية للكبد لدى الفئران، وتوضيح المسارات الجزيئية التي تُؤثّر فيها. أُجريت تجارب التسمم الفموي للفئران بشكلين مختلفين من جسيمات أكسيد الألومنيوم النانوية (Al2O3) (كرات جسيمات نانوية - NPS) وقضبان جسيمات نانوية - NPRs)، بجرعات 20 ملغ و40 ملغ/كغ من وزن الجسم يوميًا لمدة شهرين. في نهاية الفترة التجريبية، جُمعت عينات من الدم والكبد لتحديد إنزيمات الكبد الكيميائية الحيوية وعلامات الإجهاد التأكسدي، بالإضافة إلى التقييم النسيجي للكبد. كما تم البحث في التوصيف المناعي النسيجي لـ AMPK و1-Sirt. أظهرت النتائج أن خلايا NPCs من أكسيد الألومنيوم (Al2O3) حفزت زيادة ملحوظة في إنزيمات الكبد ومعايير الإجهاد التأكسدي تبعًا للجرعة، وتغيرات نسيجية مرضية حادة في الكبد، بما في ذلك تدهن الكبد من حويصلات كبيرة إلى حويصلية صغيرة، ونخر الخلايا الكبدية، بالإضافة إلى تفاعلات ورمية حادة تميزت باعتلال الأوعية الدقيقة مع تليف القناة الصفراوية البابية. وكان انخفاض تنظيم AMPK وتعبير 1-Sirt في النسيج الكبدي واضحًا.

الكلمات الدالة: اكسيد الألومنيوم، الجسيمات النانوية، الكبد، 1-Sirt، AMPK، الفئران.